Tyrosine and Tryptophan Structure Markers in Hemoglobin Ultraviolet Resonance Raman Spectra: Mode Assignments via Subunit-Specific Isotope Labeling of Recombinant Protein†

Xuehua Hu and Thomas G. Spiro*

Department of Chemistry, Princeton University, Princeton, New Jersey 08544

Received May 14, 1997; Revised Manuscript Received September 15, 1997⊗

ABSTRACT: Phenyl-deuterated tyrosine (Tyr-d_4) and indole-deuterated tryptophan (Trp-d_5) have been selectively incorporated into hemoglobin (Hb) by expressing the gene in auxotrophic strains of *Escherichia coli*. Ultraviolet resonance Raman (UVRR) spectra, using 229-nm excitation, show that difference features characteristic of the Hb quaternary R → T transition are not perturbed by the incorporation of the isotopes. All the UVRR bands between 800 and 1700 cm^{-1} are assigned to either Tyr or Trp except for the 1511 cm^{-1} band, which had been thought to arise from the Trp 2 × W18 overtone. This band does not shift upon Trp or Tyr labeling but does shift 5 cm^{-1} in D_2O, suggesting assignment to a histidine (His) residue. Its intensification in the T-state is consistent with His protonation. The α- and β-subunits were selectively labeled, by reconstitution of labeled subunits with unlabeled subunits, to make isotope hybrids. Selective Tyr labeling identified the α subunits as the locus of the Y8a upshift observed in Hb, supporting the previous inference that this shift is associated with the T-state H-bond involving the interfacial Tyr α42 [Rodgers, Su, Subramaniam, & Spiro (1992) *J. Am. Chem. Soc. 114,* 3697]. Selective Trp labeling showed the Trp α14 contributions to the T − R difference spectrum to be negligible and confirmed Trp β37 as the locus of the W3 difference signal, and probably of the remaining Trp signals as well. The observed downshift of W17 and upshift of Wd5 in the T-state are consistent with a stronger T-state H-bond between Trp β37 and Asp α94; the resulting excitation profile red shift accounts for the dominance of the Trp β37 contribution to the T − R difference UVRR spectrum.

The advent of reliable ultraviolet lasers has made it possible to use ultraviolet resonance Raman (UVRR)[1] spectroscopy to selectively probe the environments of aromatic side chains in proteins [Harada & Takeuchi, 1986; Hudson & Mayne, 1987; Su *et al*., 1989; Kitagawa, 1992; Rodgers *et al*., 1992, Jayaraman & Spiro, 1995; for a recent review see Austin *et al*. (1993)]. Recently our group and others have examined the UVRR spectra of human hemoglobin (Hb), a protein widely studied as a paradigm of allostery and cooperativity, in its high- and low-affinity states, T and R, respectively (Rodgers *et al*., 1992; Jayaraman *et al*., 1993; Mukerji & Spiro, 1994; Cho *et al*., 1994; Jayaraman & Spiro, 1995; Nagai *et al*., 1995; Hirsch *et al*., 1996). The 230-nm-excited T minus R difference spectra contain prominent signals from both tyrosine (Tyr) and tryptophan (Trp) residues (Rodgers *et al*., 1992). These UVRR markers of the R → T transition were attributed to conformational changes of the residues at the $\alpha_1\beta_2$ and $\alpha_2\beta_1$ interfaces, especially Trp β37 and Tyr α42 (Figure 1). It has also been demonstrated that a difference band at 1511 cm^{-1} can be used as a quantitative T-specific spectroscopic indicator (Mukerji & Spiro, 1994). The calculated T-fractions in cyanomet-Hb valency hybrids were in excellent agreement with those estimated previously from the biphasic time course of CO binding (Cassoly & Gibson, 1972).

Of particular importance are the Trp W3 bands at 1550−1560 cm^{-1}; different W3 components exhibit quite different evolutions in time-resolved UVRR difference spectra (Rodgers & Spiro, 1994). A specific W3 assignment was made for Trp β37 using Hb Rothschild, a natural Hb mutant with Trp β37 replaced by arginine (Rogers *et al*., 1992). However, it is necessary to make definitive assignments of all the bands in order to increase confidence in the structural interpretation of the spectra. There are three Trp and six Tyr residues per $\alpha\beta$ dimer, and they all contribute to the UVRR scattering.

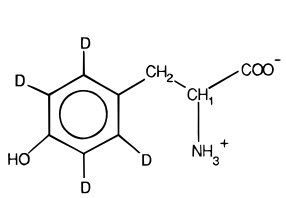

I

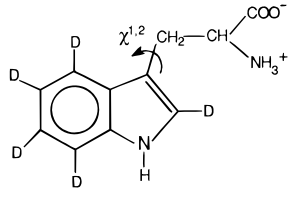

II

In order to extend available assignments we have taken advantage of a bacterial expression system for fully func-

† This work was supported by NIH Grant GM 25158 from the National Institute of General Medical Sciences.

* Author to whom correspondence should be addressed.

⊗ Abstract published in *Advance ACS Abstracts,* November 15, 1997.

[1] Abbreviations: Hb, hemoglobin; HbA, adult human hemoglobin; rHb, recombinant hemoglobin; Tyr-d_4, phenol-ring-deuterated tyrosine; rHb-Y-d_4, recombinant hemoglobin labeled with phenol-ring-deuterated tyrosine; $(\alpha_{DY}\beta_A)_2$, isotope hybrid hemoglobin with only α-subunits labeled with phenol-ring-deuterated tyrosine; $(\alpha_A\beta_{DY})_2$, isotope hybrid hemoglobin with only β-subunits labeled with phenol-ring-deuterated tyrosine; Trp-d_5, indole-ring-deuterated tryptophan; rHb-W-d_5, recombinant hemoglobin labeled with indole-ring-deuterated tryptophan; $(\alpha_{DW}\beta)_{A2}$, isotope hybrid hemoglobin with only α-subunits labeled with indole-ring-deuterated tryptophan; $(\alpha_A\beta_{DW})_2$, isotope hybrid hemoglobin with only β-subunits labeled with indole-ring-deuterated tryptophan; UVRR, ultraviolet resonance Raman.

S0006-2960(97)01136-7 CCC: $14.00

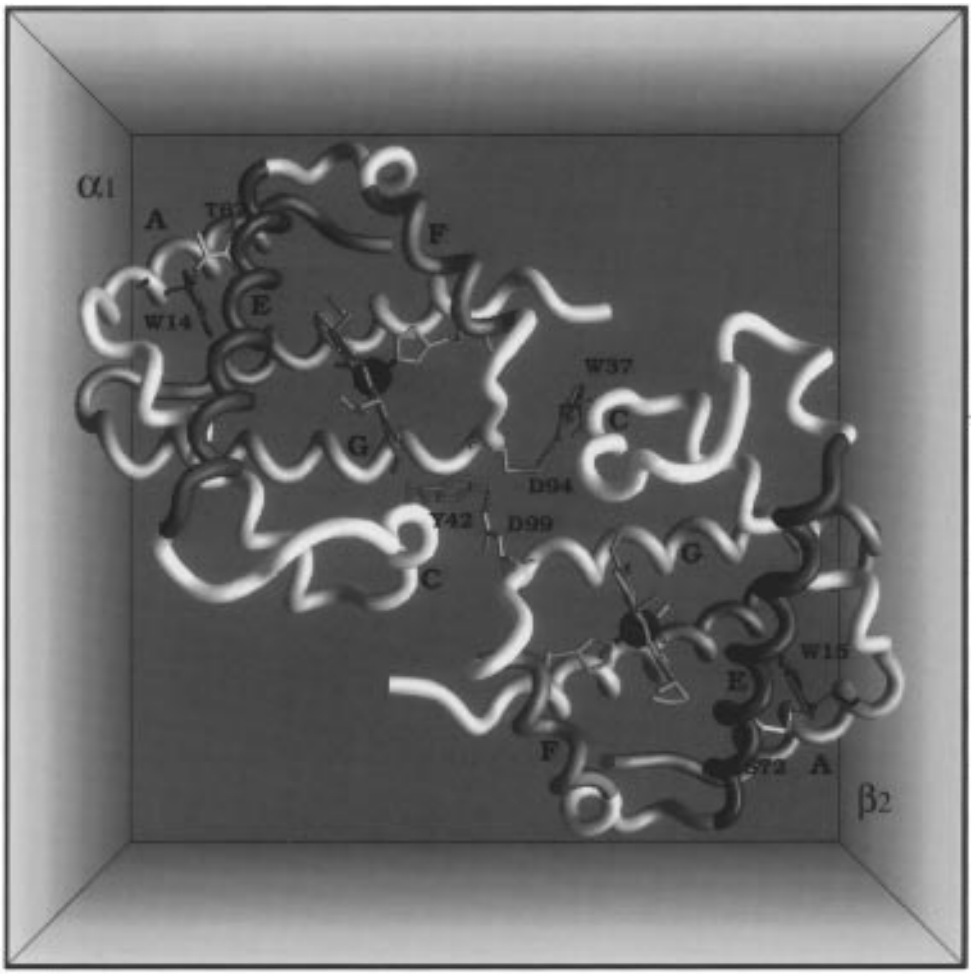

FIGURE 1: Helix diagram of the α_1 and β_2 subunits of deoxy-Hb (from crystallographic coordinates of deoxy-HbA; Fermi *et al*., 1984), showing the Trp β37−Asp α94 and Tyr α42−Asp β99 interactions at the "flexible joint" and "switch" of the $\alpha_1\beta_2$ interface, respectively. The internal Trp residues α14 and β15 are also shown with their H-bonding partners (Jayaraman *et al*., 1995).

tional Hb (Shen *et al*., 1993) to incorporate the isotopically labeled aromatic residues Tyr-d_4 (I) and Trp-d_5 (II) into Hb, using auxotrophic strains of *Escherichia coli*. Deuteration shifts the frequencies of the aromatic ring vibrations, establishing their assignments and resolving overlapped bands. Although all the Tyr or Trp residues are labeled in the expressed protein, we have been able to resolve the individual chain contributions to the UVRR spectra by separating the labeled chains and recombining them with unlabeled chains, to produce isotope hybrids. Together with the available structure parameters, these hybrids help establish the origin of the various spectral features. In addition, the labeling has revealed that the important 1511 cm^{-1} difference band does *not* arise from tryptophan, as had previously been inferred (Rodgers *et al*., 1992). However, it shifts 5 cm^{-1} in D_2O, suggesting assignment to protonated histidine.

MATERIALS AND METHODS

Plasmids, Strains, and Media. The recombinant human hemoglobin (rHb) expression plasmid pHE2 containing synthetic α- and β-globin genes and *E. coli* methionine aminopeptidase (MAP) (Shen *et al*., 1993) was kindly supplied by Professor Chien Ho. In order to efficiently incorporate isotopically labeled amino acids into the protein, the plasmid was transformed into two host cells: *E. coli* DL39 (DE3), which is auxotrophic for the six amino acids Tyr, Asp, Phe, Leu, Ile, and Val (LeMaster & Richards, 1988), and *E. coli* KS463 (DE3) (B. Konrad strain, obtained from *E. coli* Genetic Stock Center at Yale University), which is auxotrophic for Trp. Natural abundance rHb was expressed by growing the bacteria in Luria−Bertani (LB) medium. Expression was induced by adding isopropyl β-D-thiogalactopyranoside (IPTG, Sigma) to a concentration of 50 mg/mL when the cell density reached $OD_{600} = 1$. At the time of induction the culture was supplemented with hemin (20 mg/L, Sigma). Six hours after induction, the cells were harvested by centrifugation and then stored frozen at 77 K until needed for purification.

To produce specifically Tyr-d_4-labeled hemoglobin (rHb-Y-d_4), the host cell DL39(DE3) was grown in a defined M9 medium supplemented with 20 amino acids. Tyr-d_4 was supplied at a minimal level for sufficient cell growth, which was about 25% of the concentration normally used in the defined medium (LeMaster & Richards, 1985). Specifically, the medium contained 40 mg of L-Tyr-d_4 (98%, purchased from Cambridge Isotope Laboratories) and appropriate unlabeled L-amino acids (0.50 g of Ala, 0.40 g of Arg, 0.40 g of Asn, 0.40 g of Asp, 0.05 g of Cys, 0.40 g of Gln, 0.65 g of Glu, 0.55 g of Gly, 0.10 g of His, 0.23 g of Ile, 0.23 g of Leu, 0.42 g of LysHCl, 0.25 g of Met, 0.13 g of Phe, 0.10 g of Pro, 2.10 g of Ser, 0.23 g of Thr, and 0.23 g of Val), as well as 0.50 g of adenine, 0.65 g of guanosine, 0.20 g of thymine, 0.50 g of uracil, 0.20 g of cytosine, 1.50 g of

sodium acetate, 1.50 g of succinic acid, 0.50 g of NH_4Cl, 0.85 g of NaOH, and 10.5 g of K_2HPO_4 per 950 mL of water. After autoclaving, 50 mL of 20% glucose, 2 mL of 1 M $MgSO_4$, 1 mL of 0.01 M $FeCl_3$, 0.2 mL of 0.1 M $CaCl_2$, and 2 mg of $ZnCl_2$, 2 mg of $MnCl_2$, 50 mg of thiamin, 50 mg of Trp, and 50 mg of ampicillin were adeed under sterile conditions. The Trp-d_5-labeled hemoglobin (rHb-W-d_5) was produced by expression of host cell KS463 (DE) in a similar defined M9 medium except that the 50 mg of L-Trp and 40 mg of L-Tyr-d_4 were replaced by 30 mg of L-Trp-d_5 (98%, Cambridge Isotope Laboratories) and 0.17 g of L-Tyr.

Purification of Hbs. The protocol to purify the rHb and Hb-Y-d_4 or rHb-W-d_5 was based upon the procedures of Looker *et al*. (1994) and Shen *et al*. (1993) with some modifications. Frozen cells were thawed and resuspended in lysis buffer (20 mM Tris·HCl/1 *m*M benzamidine; about 3 mL/g of cells). Lysozyme was added to give 1 mg of lysozyme/g of cells. The mixture was stirred occasionally and incubated at room temperature for about 15 min. Then $MgCl_2$, $MnCl_2$, and deoxyribonuclease (DNase I, Sigma) were added to final concentrations of 10 mM, 1 mM, and 30 μg/mL, respectively. The lysate was sonicated in an ice bath at 70 W twice for 4 min and centrifuged at 14 000 rpm for 45 min to remove cell debris. The supernatant was exposed to CO gas, the pH was adjusted to 7.4 using 1 M Tris base, and 10% poly(ethylenimine) (w/v) was added to a final concentration of 0.2% to precipitate out most nucleic acids. The mixture was stirred and then centrifuged at 14 000 rpm for another 45 min. The supernatant was concentrated and adjusted to pH 7.4.

Four columns were used in the final purification process. The lysate was loaded on a Q-Sepharose fast-flow anion exchanger (Pharmacia) with 20 *m*M Tris·HCl/0.1 *m*M triethylenetetraamine (TETA), pH 7.4. The eluent was concentrated and then loaded onto a second Q-Sepharose fast-flow anion exchanger. The column was washed with buffer (20 *m*M Tris·HCl/0.1 *m*M TETA, pH 8.3) until no further nucleic acid was eluted out. Then a 160 *m*M NaCl gradient in the same buffer was used to elute out the rHb. The third column was an SP-Sepharose fast-flow cation exchanger (Pharmacia) with a gradient of 10 *m*M potassium phosphate/0.1 *m*M EDTA, pH 6.8, to 20 *m*M potassium phosphate/0.1 *m*M EDTA, pH 8.3. Recombinant Hb was collected and passed though the last column, G-75. Finally, the protein was oxidized and then reduced back to its CO form 1 day later. Typically, 7−10 mg of pure protein was obtained from 1 L of LB or defined M9 medium. All manipulations of Hbs were done at 4 °C.

Adult human hemoglobin (HbA) was prepared from fresh human blood following standard procedures (Antonini & Brunori, 1971). All the proteins were stored frozen at 77 K as the CO derivative until needed. Solutions (1 *m*M in heme) were prepared in 50 *m*M phosphate buffer at pH 7.4 when UVRR spectra were taken. Deoxy Hb was generated by photolysis of HbCO with continuous white-light illumination at 4 °C under nitrogen. The same sample was reconverted to HbCO by exposure to CO when the UVRR spectra of HbCO were taken. $NaClO_4$ (0.2 M) was added to the sample as an internal standard.

Separation and Assembly of the α- *and* β-*Subunits.* The α- and β-subunits of HbA and rHb were separated following the published procedure of Ikeda-Saito *et al*. (1981). Briefly, Hb in the CO form was treated with *p*-chloromercuribenzoate (p-MB), and the α- and β-subunits were separated on a DEAE-52 (Whatman) anion exchanger column. The -SH groups were regenerated by incubation of α-pMB or β-pMB subunits with dithiothreitol (Sigma) in the presence of catalase (Sigma). α-Subunits were mixed with a 1.2-fold excess of β-subunits to reconstitute tetrameric Hb, and the excess β-subunits were removed by use of a CM-52 (Whatman) cation exchanger column. The purity of both the separated subunits and the regenerated tetramer was assessed with nondenaturing 8% polyacrylamide gel electrophoresis (Bollag & Edelstein, 1991).

UVRR Spectroscopy and Mass Spectrometry. UVRR spectroscopy was carried out as previously described with minor changes (Rodgers *et al*., 1992). An intracavity doubled argon ion laser (Coherent, Innova 300 FReD) was used to generate a 229-nm continuous-wave (cw) laser line. The laser power at the sample was about 0.35 mW. An *f*/1 paraboloid mirror collected the scattered light in a 135° backscattering geometry. An *f*-matching lens focused this scattered light onto the entrance slit (150 μm slit width) of a 1.26 m single spectrometer (SPEX1269). Typically 1 h of collection was enough to produce a high-quality spectrum. The spectral intensities were normalized by adjusting the heights of the 934 cm^{-1} band of 0.2 M $NaClO_4$, added as an internal standard to the solutions. The normalized spectrum of HbCO was subtracted from that of deoxy-Hb to generate the difference spectrum.

Mass spectra were obtained at the Washington University Mass Spectrometry Resource, using a VG-ZAB-T four-sector mass spectrometer with VG electrospray ionization source.

RESULTS

Recombinant Hb. The rHb from the pHE2 expression system was extensively characterized by Ho and co-workers, using ^{1}H NMR spectroscopy (Shen *et al*., 1993). They reported that the rHb could be separated into two major peaks via Mono S column chromatography. The rHb in one of the peaks had an altered heme conformation in the β chain, presumably due to improper heme insertion into the globin. The aberrant properties disappeared if the rHb was converted to the ferric state and back to the ferrous form before ligation with either O_2 or CO. Consequently we cycled all rHb preparations to the ferric state for 1 day and back to the deoxy form before conversion to the CO adduct, in order to ensure proper heme insertion into the globin molecules.

The resulting preparations had UVRR spectra identical to those of native HbA, as illustrated in Figure 2. Excitation at 230 nm enhances several Tyr and Trp ring modes, which differ slightly in position and/or intensity for deoxy-Hb and HbCO (Rodgers *et al*., 1992). Digital subtraction produces a characteristic difference spectrum, which is essentially indistinguishable for rHb and native Hb, even at 5× scale expansion (Figure 2). Thus we can be confident that the results of labeling rHb are fully applicable to the Hb spectrum.

Another identity test was provided by electrophoresis in nondenaturing polyacrylamide gels. As shown in Figure 3, rHb-Y-d_4 ran at the same rate (lane 6) as native HbA (lane 1). So did the Tyr isotope hybrids (lanes 4 and 5), reconstituted from separated chains of native HbA and of tyrosine-labeled rHb. The separated chains themselves ran at different rates (lane 2, α chains; lane 3, β chains). The

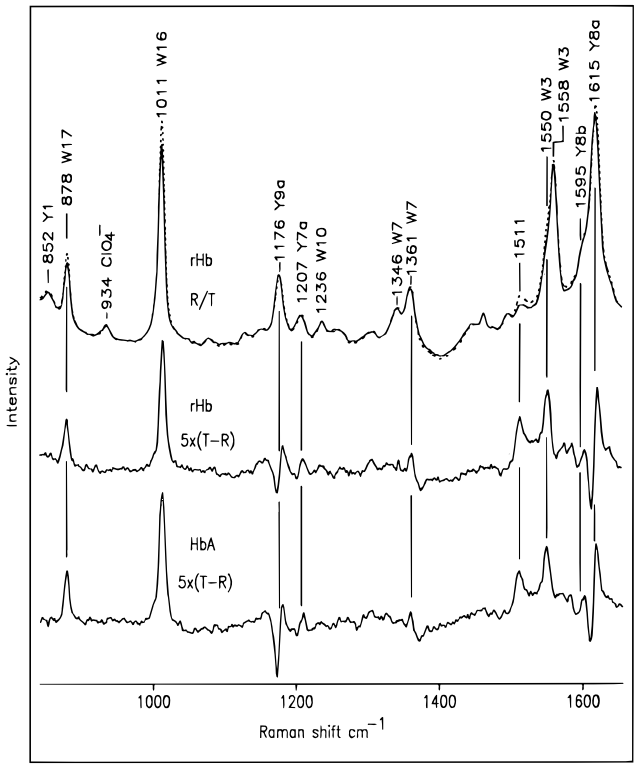

FIGURE 2: 229 nm excited UVRR spectra of deoxy-rHb (T-state, dotted top trace) and rHbCO (R-state, solid top trace), and the T − R difference spectrum multiplied by a *y*-scale factor of 5 (middle trace). Shown for comparison is the corresponding difference spectrum of HbA (bottom trace).

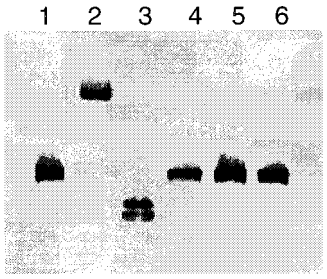

FIGURE 3: Nondenaturing polyacrylamide gel analysis of assembled hybrids in their CO forms (Bollag & Edelstein, 1991). The separating gel was 8% acrylamide/0.375 M Tris, pH 8.8, and the stacking gel was 5% acrylamide/0.125 M Tris, pH 6.8. The electrode buffer was 0.025 M Tris/0.192 *M* glycine, pH 8.3, and the electrophoresis was run at 4 °C and 200 V for 60 min. Gel was stained with Coomassie Brilliant Blue: HbA (lane 1); α-SH (lane 2); *β*-SH (lane 3); isotope hybrid $(\alpha_A\beta_{DY})_2$ (lane 4); isotope hybrid $(\alpha_{DY}\beta_A)_2$ (lane 5), and rHb-Y-d_4 (lane 6).

same results were obtained with the tryptophan-labeled rHb hybrids. Thus the reconstitution procedure produced nativelike tetramers.

Tyr-d_4-Labeled Recombinant Hb. Mass spectroscopy revealed clean incorporation of Tyr-d_4 into rHb via the *E. coli* DL39 (DE3) auxotroph (Table 1). Since each chain has three Tyr residues, labeling should increase its mass by 12 amu, which is within experimental error of the observed increases of 12 for α chains and 11 for *β* chains. Likewise the UVRR spectra (Figure 4) reveal complete replacement of the Tyr bands with those characteristic of Tyr-d_4 (Figure 5). For example, essentially no intensity is left at the position of the prominent Y9a band, which is shifted out of the region in Tyr-d_4.

Table 1: Masses of rHb-Y-d_4, rHb-W-d_5, and rHb Measured by Electrospray Mass Spectrometry[a]

	Tyr-d_4		Trp-d_5	
	α chain	*β* chain	α chain	*β* chain
isotope-labeled	15139	15879	15131	15877
nonlabeled (rHb)	15127	15868	15127	15868
measured difference	12	11	4	9
expected difference[b]	12	12	5	10

[a] Listed here are the two major peaks. Very small peaks corresponding to larger masses were also observed. The calculated masses of rHb are 15 126 and 15 867 for the α and *β* chains, respectively. [b] There are three Tyr residues on each chain, and d_4 substitution adds 12 amu. Trp-d_5 substitution adds 5 amu to the α chain, which has one Trp residue, and 10 amu to the *β* chain, which has two Trp residues.

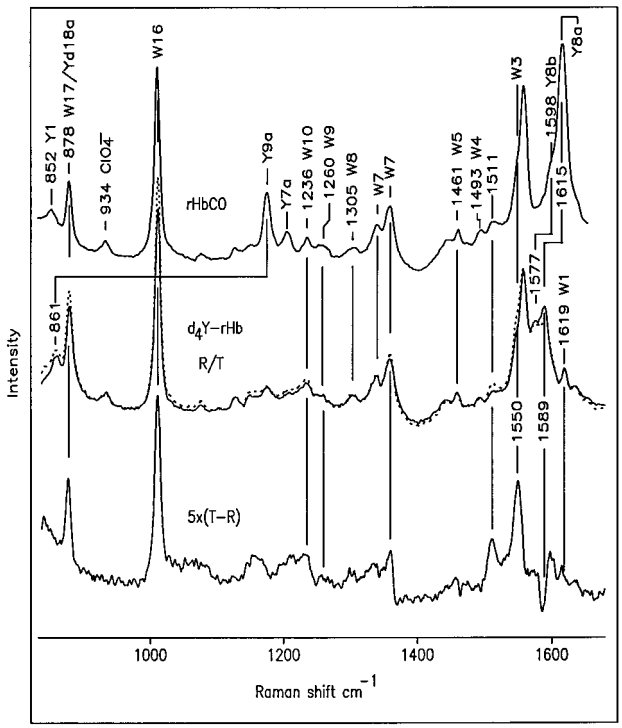

FIGURE 4: 229 nm excited UVRR spectra of deoxy-rHb-Y-d_4 (T-state, dotted middle trace) and its CO adduct (R-state, solid middle trace), and the T − R difference spectrum multiplied by a *y*-scale factor of 5 (bottom trace). Shown for comparison is the UVRR spectrum of rHbCO (top trace).

The Tyr and Tyr-d_4 assignments (Y*i* and Yd*i*, where *i* is the mode number) are based on previous studies (Rava & Spiro, 1985; Takeuchi *et al*., 1988). The ring deuteration produces changes in relative band intensities, as well as frequencies (Figure 5). We note particularly the intensification of the Yd8b shoulder on the Yd8a band, and also the lack of enhancement for Yd7a in Tyr-d_4 and for Y7a′ in Tyr [the indicated positions are taken from nonresonance Raman data (Takeuchi *et al*., 1988)]. When the rHb-Y-d_4 spectra are examined (Figure 4), the bands are seen to be unaltered from those of HbA, except for the shifted Tyr-d_4 bands, which are all at the expected positions. Curiously, the Yd8a/d8b bands of rHb-Y-d_4 are appreciably weaker (compare the intensity of the nearby W3 band) than the Y8a/8b bands of rHb, although this is not expected from the aqueous Tyr and Tyr-d_4 spectra (Figure 5). We speculate that the altered mode compositions in Tyr-d_4 produce subtle changes in the excitation profile, leading to environmental sensitivity (water vs the protein interior) of the relative band intensities.

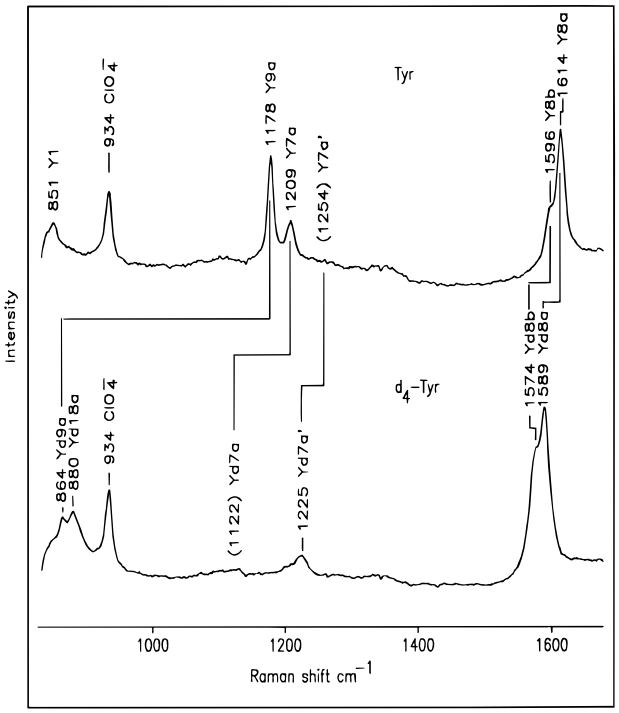

FIGURE 5: 229 nm excited UVRR spectra of aqueous amino acids Tyr and Tyr-d_4 at 1 *m*M concentration in 50 *m*M phosphate buffer (pH 7.4), The positions of unobserved bands (parentheses) are taken from nonresonant Raman spectra of the model compounds *p*-cresol and *p*-cresol-2,3,5,6-d_4 (Takeuchi *et al*., 1988).

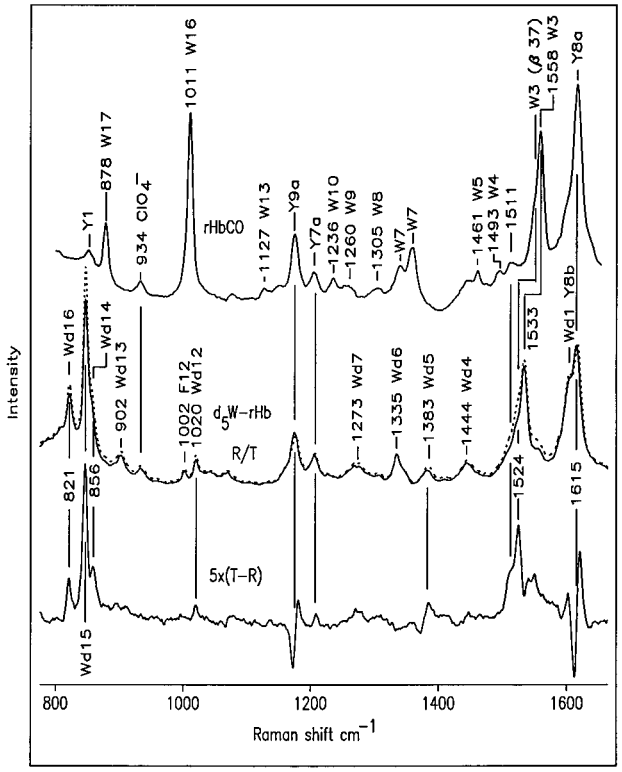

FIGURE 6: 229 nm excited UVRR spectra of deoxy-rHb-W-d_5 (T-state, dotted middle trace) and its CO adduct (R-state, solid middle trace) and the T − R difference spectrum multiplied by a *y*-scale factor of 5 (bottom trace). Also shown for comparison is the UVRR spectrum of rHbCO (top trace).

The deoxy minus CO difference spectrum of rHb-Y-d_4 reveals a sigmoidal band at the shifted Yd8a position (1589 cm^{-1}), which has the same shape as the Y8a difference band of HbA (Figure 2) but with lower amplitude. The other characteristic Tyr difference band, Y9a, is missing for rHb-Y-d_4, because of its large frequency shift. (The position of Yd9a is at the edge of the spectrum, where its contribution to the difference spectrum is unclear.) The Trp difference bands are all unaltered in position, shape, and amplitude from the HbA difference spectrum.

The shift in Yd8a reveals an additional Trp band, W1 (see Figure 7), at 1619 cm^{-1} (Figure 4). Its amplitude is low, and it does not contribute significantly to the difference spectrum. In addition, the shift in Yd8a reveals that there is no additional contribution from Phe (phenylalanine) residues, whose F8a band is expected at 1606 cm^{-1} (Fodor *et al*., 1989). These conclusions remove a significant uncertainty in the interpretation of the HbA difference spectrum (Rodgers *et al*., 1992); the Y8a difference band reflects environmental influences on Tyr residues only, without interference from Trp or Phe.

Trp-d_5-Labeled Recombinant Hb. The mass spectrum (Table 1) likewise shows quantitative incorporation of Trp-d_5 into rHb via the *E. coli* KS463 (DE3) auxotroph. The mass increases, 4 and 9, for the α and β chains, are within experimental error of those expected for labeling of one and two Trp residues. Likewise, the UVRR spectra (Figure 6) reveal clean incorporation of label. Thus, no intensity is left at the position of the strongest Trp band, W16 (1011 cm^{-1}), in the rHb-W-d_5 spectrum. Instead, one can now see a very small band at 1002 cm^{-1}, which is attributable to the Phe F12 band. This is the strongest band in the Phe UVRR spectrum at 230 nm excitation (Fodo *et al*., 1989), and its weakness confirms the absence of significant Phe contributions to any of the 230-nm-excited bands. RR enhancement becomes strong for Phe near 200 nm (Fodor *et al*., 1989) but is weak at 230 nm. Thus, even though there are many more Phe residues (15 per dimer) than either Tyr or Trp, they do not interfere at this wavelength.

The UVRR spectra of Trp and of Trp-d_5 are complex (Figure 7). Not only does indole ring deuteration shift the frequencies, but it alters the mode compositions so that the intensity distribution is quite different. Thus, the 1342/1360 cm^{-1} W7 Fermi doublet (Harada & Takeuchi, 1986) disappears on deuteration and its intensity best correlates with Wd6, at 1334 cm^{-1} [see Maruyama and Takeuchi (1995) for the assignment scheme]. Likewise, the strong 1012 cm^{-1} W16 band disappears, and its intensity reappears in the 849 cm^{-1} Wd15 band and its 863 cm^{-1} Wd14 shoulder. Also, W17 (880 cm^{-1}) correlates with Wd16 (821 cm^{-1}). Fortunately, the important W3 band at 1552 cm^{-1} is easily recognizable at its shifted Wd3 position, 1525 cm^{-1}. Finally, we note the presence of shoulders at the expected positions of two higher-order modes: the 2 × W18 overtone (1514 cm^{-1}) and the W17 + W18 combination (1637 cm^{-1}). These assignments are supported by the absence of features at 1514 or 1637 cm^{-1} for Trp-d_5 (Figure 7), in which the fundamental frequencies are shifted strongly. Detection of these two particular higher-order modes is not unexpected since W18 is the strongest band the Trp UVRR spectrum.

The Trp-d_5 bands all appear at the expected positions in the rHb-W-d_5 spectrum (Figure 6), leaving the Tyr bands unchanged (except that the shifted Wd1 band adds to the apparent intensity of the Y8b band). We note, however, that the weak broad band at 1260 cm^{-1}, which had been assigned to the Tyr mode Y7a′ by Cho *et al*. 1994), is missing in the rHb-W-d_5 spectrum and is assigned to W9 instead.

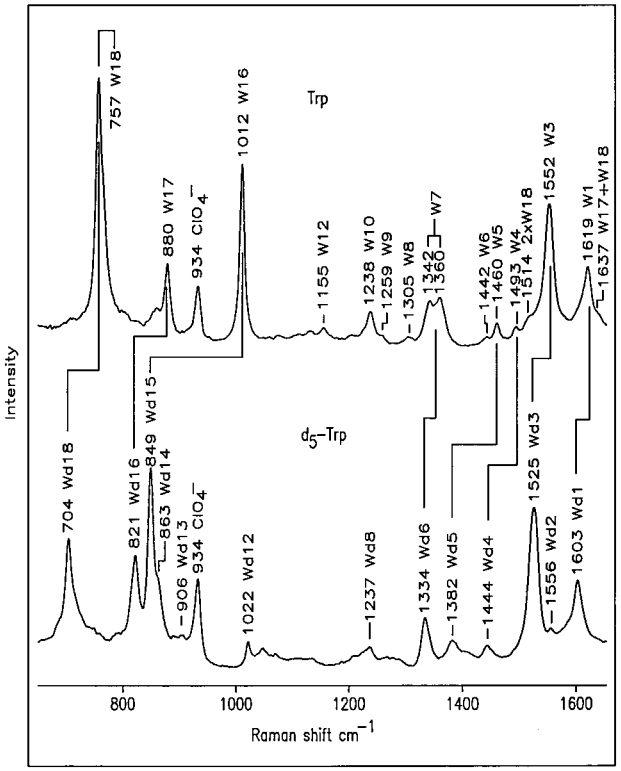

FIGURE 7: 229 nm excited UVRR spectra of aqueous amino acids Trp and Trp-d_5 at 1 *m*M concentration in 50 *m*M phosphate buffer (pH 7.4).

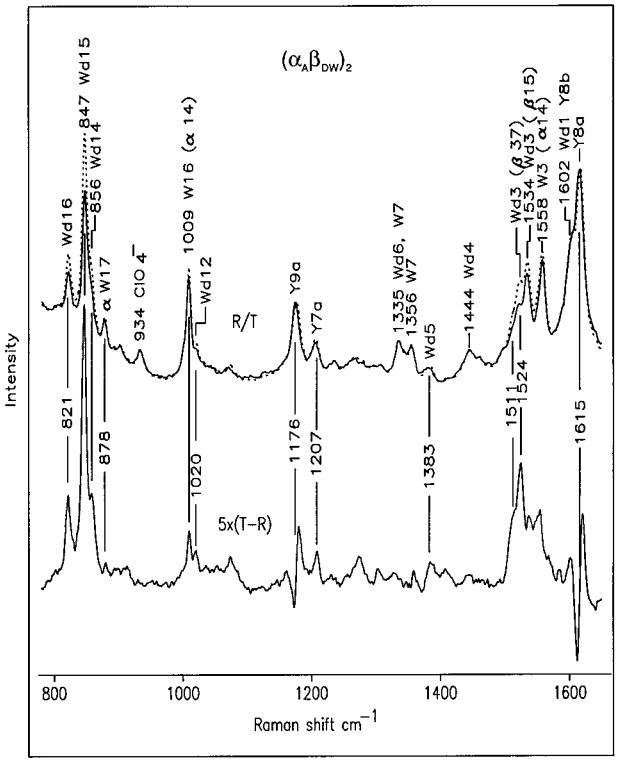

FIGURE 8: 229 nm excited UVRR spectra of the tryptophan isotope hybrid $(\alpha_A\beta_{DW})_2$ in the deoxy form (T-state, dotted top trace) and CO form (R-state, solid top trace) and the T − R difference spectrum multiplied by a *y*-scale factor of 5 (bottom trace).

In the deoxy minus CO difference spectrum (Figure 6), the Tyr bands are the same as those seen for HbA, but a new set of Trp difference bands is seen. As expected, the positive difference bands for W17 and W16 are replaced by positive difference bands for Wd16 and Wd15/d14. Interestingly, the sigmoidal difference band for W7 (1361 cm^{-1}, Figure 2), is replaced by another sigmoidal feature, but of opposite sense, for Wd5 (1383 cm^{-1}). The Wd3 difference band is at 1524 cm^{-1}, which is at the position of the low-frequency shoulder on the main Wd3 band (1533 cm^{-1}), just as it is in the unlabeled protein (Rodgers *et al*, 1992).

Trp Isotope Hybrids $(\alpha_A\beta_{DW})_2$ *and* $(\alpha_{DW}\beta_A)_2$. The Trp isotope hybrids permit unambiguous identification of the Trp α14 contribution, since this is the only Trp residue in the α chains, while the β chains contain two Trp residues, β37 and β15. Consistent with this composition, roughly a third of the rHb intensity remains at the W*i* (natural abundance) positions when the β-chain Trp residues are labeled [$(\alpha_A\beta_{DW})_2$, Figure 8], while about a third of the W*i* intensity is shifted to the Wd*i* positions when the α-chain is labeled [$(\alpha_{DW}\beta_A)_2$, Figure 9].

In the case of W3, the separation of the Trp β37 contribution into a low-frequency shoulder (Rodgers *et al*., 1992) permits the positions and intensities of all three residues to be resolved (Figure 10 and Table 2). The Trp α14 and β15 bands are found at nearly the same frequency and have about the same intensity, as had earlier been assumed (Rodgers *et al*., 1992). Conversion from the R- to the T-state results in very small increases in intensity (∼5%) and slight frequency shifts, +0.4 cm^{-1} for Trp β15 and −0.5 cm^{-1} for Trp α14. In the case of Trp β37, the T − R frequency shift is likewise slight, +0.5 cm^{-1} (although the Wd3 shift is +1.8 cm^{-1}), but the intensity increase is large, 31% (50% for Wd3). This is the reason that the W3

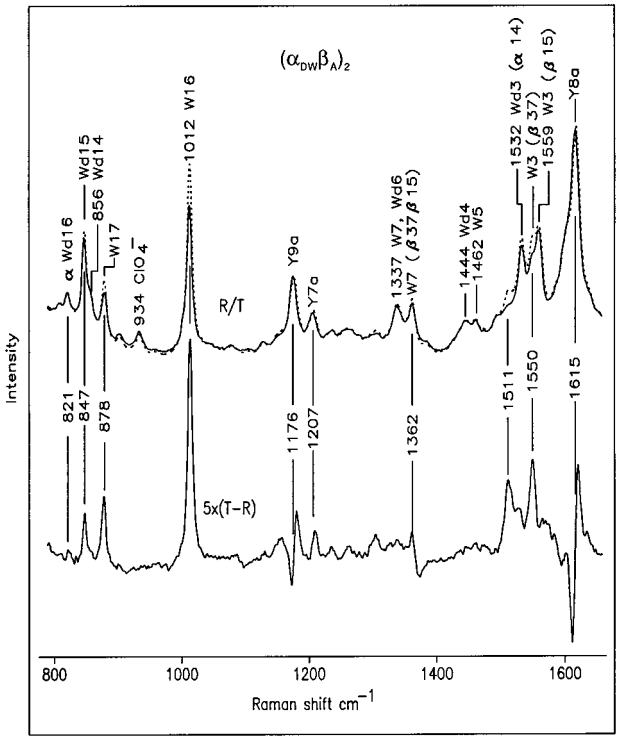

FIGURE 9: 229 nm excited UVRR spectra of the tryptophan isotope hybrid $(\alpha_{DW}\beta_A)_2$ in the deoxy form (R-state, dotted top trace) and CO adduct (R-state, solid top trace) and the T − R difference spectrum multiplied by a *y*-scale factor of 5 (bottom trace).

contribution to the difference spectrum is almost entirely from Trp β37 (Figures 8 and 9) (Rodgers *et al*., 1992).

The W3 frequency is known to depend on the dihedral angle, $\chi^{2,1}$, about the bond connecting the indole ring with the C_β atom (Miura *et al*., 1989). The frequency is lower

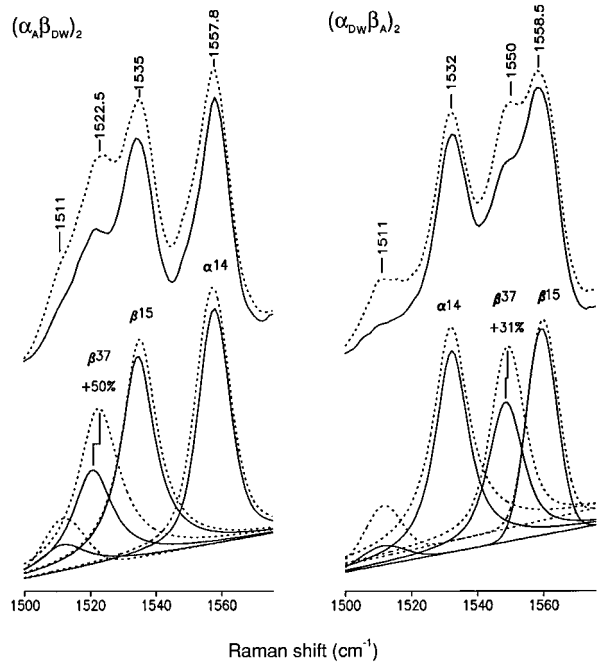

FIGURE 10: Band deconvolution in the W3 region (1500−1570 cm^{-1}) for (left panel) deoxy hybrid $(\alpha_A\beta_{DW})_2$ (T-state, dotted traces) and its CO adduct (R-state, solid traces) and for (right panel) deoxy hybrid $(\alpha_{DW}\beta_A)_2$ (T-state, dotted traces) and its CO adduct (R-state, solid traces). Shown at the top are the original spectra for both R- and T-states.

for Trp β37 than for Trp β15 and α14 because of its distinctly lower $\chi^{1,2}$ (Rodgers *et al*., 1992). Equations describing this empirical relationship, for both W3 and Wd3, have recently been given by Maruyama and Takeuchi (1995), and the predicted frequencies are listed in Table 2. They agree very well with the experimental values for Trp β37 and α14, while small deviations (∼5 cm^{-1}) are found for Trp β15. The predicted T − R frequency change is also in excellent agreement with experiment for Trp β37 but is somewhat larger (3−4 cm^{-1}) than observed for Trp β15 and α14.

The W16 and W17 bands, which give rise to large difference signals, have also been deconvoluted into α- and β-chain contributions (Table 3). The band overlaps do not permit separation of the Trp β37 and β15 contributions, although the larger deconvolution bandwidths required for the β-chains than for the α-chains indicate that the β37 and β15 frequencies are not identical. The T − R frequency changes are small, but the −0.4 cm^{-1} W17 shift for Trp β37/15 is outside experimental error. We attribute this shift to stronger H-bond donation by the Trp β37 indole NH in the T-state than in the R-state, since the H-bond acceptor is the negatively charged carboxylate of Asp β94 in the former (Figure 1) but the neutral carbonyl of Asn β102 in the latter (Table 4). The W17 frequency is known from model compounds to diminish upon indole H-bonding (Miura *et al*., 1988). Consistent with this inference is the sigmoidal difference signal for the 1383 cm^{-1} Wd5 band of the β chains (Figure 8). This band has recently been found to shift up when the Trp indole NH is an H-bond donor (Maruyama & Takeuchi, 1995). Thus, the W17 downshift and the Wd5 upshift detected in the T − R difference spectrum are both consistent with Trp β37 having a stronger H-bond partner in the T-state. It is possible that the sigmoidal difference signal seen for the 1362 cm^{-1} W7 band in the β chains (Figure 9) has the same origin, although this band, being part of the Fermi doublet, has a complex dependence on the environment of the indole ring (Harada *et al*., 1986).

For the Trp β15 and α14 residues, the H-bond acceptors (the OH groups of Ser β72 and Thr α67) are unaltered in the T and R structures. The negligible shift (+0.2 cm^{-1}) in the Trp α14 W17 frequency (Table 3) or in its Wd5 frequency (Figure 9) indicates that there is no significant change in the H-bond strength, and we infer that this is the case for Trp β15 as well.

When the W16 and W17 intensities are examined (Table 3), the T − R differences are small (∼5%) for Trp α14 but large (∼30%) for Trp β37/15. Consequently, the β-chain is responsible for most of the T − R difference signals, as can readily be confirmed by comparing the difference spectra for the two isotopic hybrids (Figures 8 and 9). Since the W16 and W17 β-chain intensity increments are similar to the W3 increment observed for Trp β37 alone (Figure 10), we infer that the T − R difference signals all arise mainly from Trp β37, with Trp β15 and α14 contributing to only a small extent.

Tyr Isotope Hybrids $(\alpha_A\beta_{DY})_2$ and $(\alpha_{DY}\beta_A)_2$. Because each chain contains three Tyr residues, the individual residue contributions cannot be separated. However, the isotope hybrids do show chain-selective effects (Figures 11 and 12), which can be interpreted with the aid of the crystallographic structures. The Y9a signal is particularly clear-cut, since the deuterium label shifts this band out of the spectral region. The unlabeled signal, in either hybrid, has about half the intensity of the original rHb/HbA signal, as expected. For both hybrids the Y9a intensity is lower in the T- than the R-state, accounting for the negative difference signal. However, the frequency is affected differently. In the T-state, the band shifts down 0.6 cm^{-1} for the β-chains (Figure 12) but up +1.6 cm^{-1} for the α-chains (Figure 11). In model compounds this band has been found to be sensitive to the dihedral angle of the Tyr OH group, shifting up in frequency when the OH bond is forced into the plane of the ring (Takeuchi *et al*., 1989). When this angle is calculated from the crystallographic coordinates (Table 5), using standard assumptions about the location of the H atoms, the OH bond is found to be well out of the plane for all residues except for Tyr α93, for which the angle is large in the R-state but only 11° in the T-state. This reorientation might account for the +1.6 cm^{-1} upshift for the α-chain Y9a band.

The other key Tyr band is Y8a, which gives rise to the large sigmoidal T − R difference signal. The isotope hybrids show this signal to result from different α- and β-chain contributions. When the α-chains remain unlabeled (Figure 11), Y8a is observed to shift up 1.8 cm^{-1} in the T-state, without change in its intensity, but it intensifies and remains unshifted when the β-chains remain unlabeled. Identification of the α-chains as the locus of the Y8a upshift supports the previous inference that this shift is associated with the T-state H-bond involving the interfacial Tyr α42 (Rodgers *et al*., 1992). Unfortunately the chain contributions from Y8b, which also shifts up in the T-state, could not be disentangled because of overlap with the downshifted Yd8a; attempts at deconvolution of these multiple overlapping bands were unsuccessful.

D_2O Exchange: Does the 1511 cm^{-1} Band Arise from Histidine? An arresting result of the isotope labeling is that it disproves the previous assignment of the 1511 cm^{-1} band to the overtone of a Trp mode, W18 (Rodgers *et al*., 1992).

Table 2: Trp Residue $\chi^{2,1}$ Angles[a] and Experimental and Predicted W3/Wd3 Frequencies

		residue β37			residue β15			residue α14		
		$\chi^{2,1}$	Trp-d_0 (cm^{-1})	Trp-d_5 (cm^{-1})	$\chi^{2,1}$	Trp-d_0 (cm^{-1})	Trp-d_5 (cm^{-1})	$\chi^{2,1}$ (deg)	Trp-d_0 (cm^{-1})	Trp-d_5 (cm^{-1})
R-state	exp[b]	92	1548.6	1520.7	115	1559.4	1534.5	122	1557.8	1532.3
	pred[c]		1549.6	1522.4		1557.1	1530.9		1557.3	1531.2
T-state	exp[b]	93	1549.1	1522.5	103	1559.8	1535.0	102	1557.3	1532.0
	pred[c]		1550.0	1522.9		1554.0	1527.5		1553.7	1527.1
T − R	exp[b]		+0.5	+1.8		+0.4	+0.5		−0.5	−0.3
	pred[c]		+0.4	+0.5		−3.1	−3.4		−3.6	−4.1
$\Delta I/I_R$[d]	(%)		+30	+50		−5%	+10		+10	+10

[a] The angles were calculated from the single-crystal X-ray coordinates in the Brookhaven Protein Data Bank of $HbAO_2$ (2.1 Å, PDB deposit code 1HHO; Shaanan, 1983) and of deoxy HbA (1.74 Å, PDB deposit code 2HHB; Fermi et al., 1984), using the program Insight II (Biosym Technologies). [b] The experimental frequencies were obtained by curve-fitting of the spectra, using bands with 50% Lorentzian and 50% Gaussian line shapes (Rodgers et al., 1992). Estimated frequency reproducibility: ±0.1 cm^{-1}. [c] Predicted from $\chi^{2,1}$ angles using the correlation equations of Maruyama and Takeuchi (1995). [d] Relative change (percent) in peak height between the T- and R-states. The estimated uncertainty is ±10%.

Table 3: Frequencies, Widths, and Intensity Changes of Trp W16 and W17 Bands in Different Subunits[a]

	W16				W17			
	α14[b]	β15, β37[c]	rHb[d]	HbA[e]	α14[b]	β15, β37[c]	rHb[d]	HbA[c]
R-state	1009.0 (8.5)	1011.8 (9.5)	1010.8 (10.2)	1010.8 (10.2)	878.7 (8.3)	878.9 (10.8)	878.8 (10.4)	879.0 (10.4)
T-state	1009.1 (8.2)	1012.2 (9.4)	1011.0 (10.2)	1011.0 (10.4)	878.9 (7.8)	878.5 (10.5)	878.7 (10.2)	878.9 (10.6)
T − R	+0.1	+0.4	+0.2	+0.2	+0.2	−0.4	−0.1	−0.1
$\Delta I/I_R$[f] (%)	+5	+30	+15	+15	+2	+30	+20	+15

[a] The frequency data were obtained by curve-fitting using bands with 50% Lorentzian and 50% Gaussian line shapes (Rodgers et al., 1992) and are given in reciprocal centimeters. Estimated frequency reproducibility: ±0.1 cm^{-1}. The widths are listed in parentheses beside the frequencies. [b] Data taken from the spectra of $(\alpha_A\beta_{DW})_2$. [c] Data taken from the spectra of $(\alpha_{DW}\beta_A)_2$. [d] From the spectra of rHb. [e] From the spectra of HbA. [f] Relative peak height changes (percent) between the T- and R-states; the estimated uncertainty is ±5% for W16 and ±10% for W17.

Table 4: Trp H-Bonding Parameters from HbA Crystallographic Coordinates[a]

	$HbAO_2$			deoxy-HbA		
residue	H-bond partner	NH···X (Å)	∠N−H−X (deg)	H-bond partner	NH···X (Å)	∠N−H−X (deg)
Trp α14	Thr α67 (OH)	1.58	172	Thr α67 (OH)	1.82	169
Trp β15	Ser β72 (OH)	2.41	160	Ser β72 (OH)	2.08	145
Trp β37	Asn β102 (CO)	1.86	164	Asp α94 (COO^-)	2.00	154

[a] Calculated from the single-crystal X-ray coordinates in the Brookhaven Protein Data Bank of $HbAO_2$ (2.1 Å, PDB deposit code 1HHO; Shaanan, 1983) and of deoxy HbA (1.74 Å, PDB deposit code 2HHB; Fermi et al., 1984) using the program Insight II. Distances and angles were obtained by placing H 1.03 Å from the indole N, along the line bisecting the C−N−C angle.

This assignment was based on the frequency match ($2 \times 757\ cm^{-1} = 1514\ cm^{-1}$), and on the intensity of W18, which is the strongest band in the Trp RR spectrum and does indeed give rise to a detectable overtone band (Figure 7). Moreover, the 1511 cm^{-1} difference band intensity seemed to scale with the W3 difference intensity, and it did reflect the T-state population (Mukerji & Spiro, 1994), making the association with Trp β37 plausible. However, W18 shifts over 50 cm^{-1} in Trp-d_5 (Figure 7), whereas the 1511 cm^{-1} difference band is unshifted for rHb-W-d_5 or the hybrids (Figure 13). Nor does it shift upon Tyr labeling (Figure 4). Consequently, this quarternary marker must arise from a residue that is *not* Trp or Tyr. In contrast, the W17 + W18 combination mode (1635 cm^{-1}) is seen weakly in all the difference spectra except for those of rHb-W-d_5 and the $(\alpha_A\beta_{DW})_2$ hybrid (Figure 13), showing that it does arise from Trp residues in the β-chain, presumably Trp β37.

There are not many candidates at 1511 cm^{-1} among the known UV-enhanced protein Raman bands. The closest match is a 1497 cm^{-1} histidine band, which intensifies upon ring protonation and is assigned to an imidazole ring deformation (Caswell & Spiro, 1986). Conceivably then, the 1511 cm^{-1} Hb difference band arises from protonation of one or more His residues in the T-state. The 14 cm^{-1} frequency difference, relative to aqueous histidine, might result from side-chain conformational effects. His RR bands are not normally seen with 229 nm excitation, since the enhancement is low (Caswell & Spiro, 1986), but there may be additional enhancement from environmental effects in the protein. The 1511 cm^{-1} band is quite weak and would scarcely be noticeable, were it not for the large relative intensity change in the T-state, which produces a marked difference signal.

Since the analogous band in aqueous imidazole shifts down 4 cm^{-1} in D_2O (Salama & Spiro, 1978), as a result of H/D exchange at the ring NH group, we examined the effect on the UVRR spectrum of incubating Hb in D_2O (Figure 14). Indeed the 1511 cm^{-1} band does shift down 5 cm^{-1} in D_2O, lending support to the proposed His assignment [and confirming that the band is *not* the W18 overtone since a 10 cm^{-1} downshift is required by the 5 cm^{-1} shift of the fundamental mode upon Trp N-deuteration (Takeuchi & Harada, 1986)]. However, confirmation via further His labeling is needed, since there are many exchangeable protons in Hb.

An alternative, but less plausible, assignment is to the amide cII vibration of a *cis*-peptide link (Jordan & Spiro, 1995). In the model compound caprolactam, this vibration

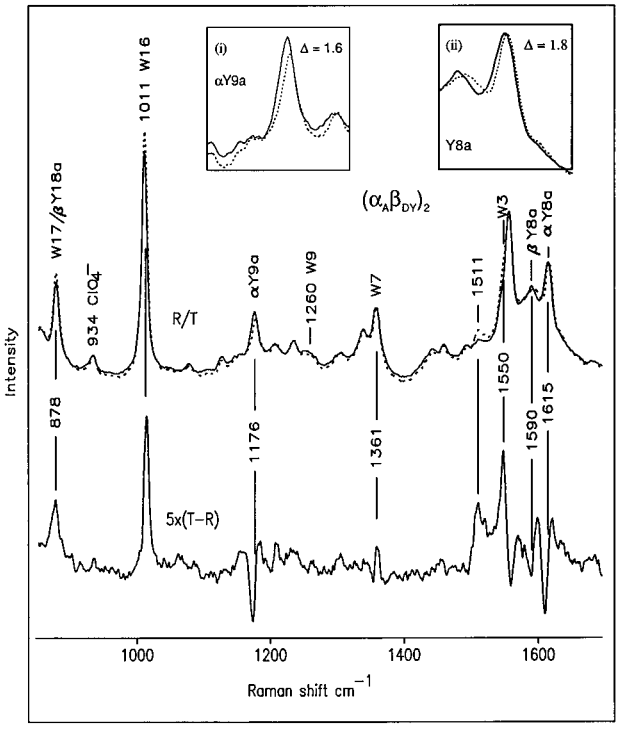

FIGURE 11: 229 nm excited UVRR spectra of the tyrosine isotope hybrid $(\alpha_A\beta_{DY})_2$ in the deoxy form (T-state, dotted top trace) and CO form (R-state, solid top trace) and their T − R differences spectrum multiplied by a *y*-scale factor of 5 (bottom trace). The insets show expanded views of the bands Y9a and Y8a.

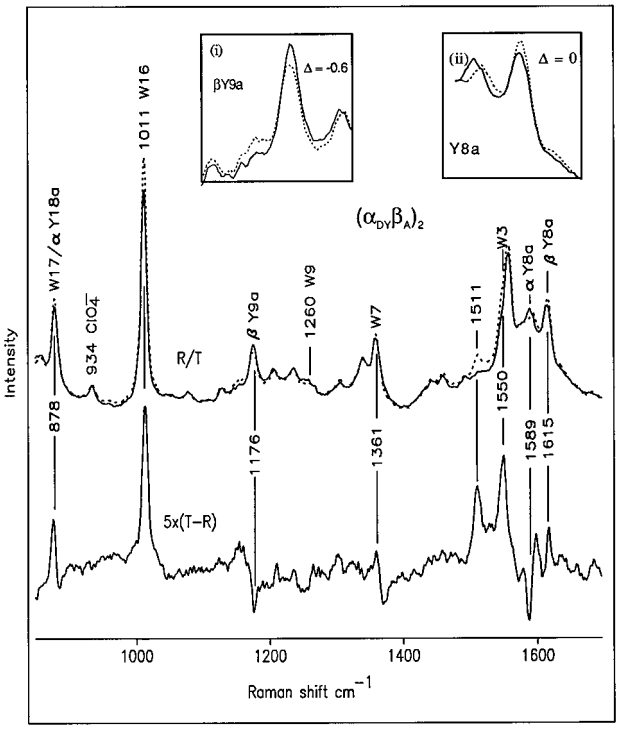

FIGURE 12: 229 nm excited UVRR spectra of the tyrosine isotope hybrid $(\alpha_{DY}\beta_A)_2$ in the dexoy form (T-state, dotted top trace) and CO form (R-state, solid top trace) and the T − R difference spectrum multiplied by a *y*-scale factor of 5 (bottom trace). The insets show expanded view of the bands Y9a and Y8a.

is located at 1492 cm^{-1} in H_2O and 1490 cm^{-1} in D_2O. But in a more constrained cyclic peptide compound, cyclo(Gly-Pro), the amide cII was found at a higher frequency, 1514 cm^{-1} in H_2O and 1503 cm^{-1} in D_2O (Takeuchi & Harada, 1990). These frequencies are close to those observed in Hb. Although the amide modes for the normal *trans*-peptide links are only enhanced strongly at wavelengths below 210 nm (Copeland *et al*., 1985), the $\pi-\pi^*$ absorption, and therefore the excitation profile, are significantly red-shifted for *cis*-peptides (Song *et al*., 1991). However, *cis*-peptide links are significantly higher in energy than *trans*-peptides and are rarely found in proteins, except in the case of proline residues. Assignment to Pro can be rejected, since its amide cII frequency is significantly lower, ∼1460 cm^{-1} (Jordan *et al*., 1996), and is insensitive to D_2O (there being no NH group in Pro). A search of the available crystallographic coordinates of oxy-Hb (Shaanan, 1983) and deoxy-Hb (Fermi *et al*, 1984), using the software PROCHECK (Laskowski *et al*, 1993), failed to reveal any *cis*-peptide in Hb, making a *cis*-peptide assignment unlikely.

D_2O also shifts several other bands in the Hb spectrum (Figure 14), since tryptophan and tyrosine both have exchangeable protons. Several Trp modes are shifted (Takeuchi & Harada, 1986) by the indole NH/D exchange, of which the most notable is W17, which has a large N−H bending contribution. Its strong UVRR enhancement and sensitivity to D_2O has been exploited to monitor H/D exchange rates for Trp residues (Liu *et al*., 1989). Two Tyr modes, Y8a and Y8b, are shifted by ∼3 and ∼14 cm^{-1}, respectively (Copeland & Spiro, 1985), because of the OH/D exchange. The larger shift of Y8b separates it from Y8a, into a clearly resolved band, at 1586 cm^{-1}. Surprisingly, however, there is no apparent frequency shift as was observed in H_2O (Rodgers *et al*., 1992) but a slight intensity gain in the T-state. It is also interesting to note that a small His III′ band around 1407 cm^{-1} (Gregoriou *et al*., 1995) was detected after H/D exchange.

DISCUSSION

Two aromatic residues, Trp β37 and Tyr α42, provide strategic probes of the important $\alpha_1\beta_2$ (and equivalently $\alpha_2\beta_2$) subunit interface, which is the locus of most of the altered quarternary contacts in Hb (Baldwin & Chothia, 1979; Baldwin, 1980). There are two separate regions for these contacts, each one between the C helix of one chain and the FG corner of the opposite chain (Figure 1). Trp β37 is on the β-chain C helix, while Tyr α42 is on the α-chain C helix. The β-C/α-FG contact region is the "flexible joint" of the interface, a kind of pivot whose reorientation between the R and T states brings a new set of contacts into play. The α-C/β-FG contact region is the "switch", where the interface helix interdigitation shifts register (Baldwin, 1980).

Flexible Joint. Some of the altered contacts in the flexible joint involve Trp β37, whose indole NH group donates an H-bond to the side chain of Asn β102 in the R-state but to the side chain of Asp α94 in the T-state (Table 4). The former provides a neutral H-bond acceptor, the amide carbonyl group, whereas the latter is presumed to be a negatively charged carboxylate acceptor, which should form a stronger H-bond. Consistent with this expectation is the −0.4 cm^{-1} downshift of W17 in the $(\alpha_{DW}\beta_A)_2$ isotope hybrid and the ∼1 cm^{-1} upshift of Wd5 in the $(\alpha_A\beta_{DW})_2$ isotope hybrid. Both shifts imply stronger H-bonding in the T-state, and both signals arise from the β-chains. The Trp β15 contribution to these shifts is expected to be small, since (i) the H-bond acceptor for Trp β15 is the same, Ser β72, in the R- and T-states, and (ii) Trp β15 and Trp α14 are

Table 5: Tyr H-Bonding Parameters from HbA Crystallographic Coordinates[a,b]

	$HbAO_2$				deoxy-HbA			
residue	H-bond partner	OH···X (Å)	∠O−H−X (deg)	∠ring-OH (deg)	H-bond partner	OH···X (Å)	∠O−H−X (deg)	∠ring-OH (deg)
Tyr α140	Val α93 (CO)	1.64	175	44	Val α93 (CO)	1.70	166	11
Tyr α42	water 49	2.03	135	81	Asp β99 COO^-	1.45	172	16
					or β99 COOH[c]	1.50	160	34/86
Tyr β145	Val β98 (CO)	1.39	171	47	Val β98 (CO)	1.57	172	27
Tyr β130	Val β11 (CO)	1.51	162	78	Val β11 (CO)	1.66	155	55
Tyr β35	none				water 80/14	2.00	166	59

[a] Calculated from the single-crystal X-ray coordinates in the Brookhaven Protein Data Bank of $HbAO_2$ (2.1 Å, PDB deposit code 1HHO; Shaanan, 1983) and of deoxy HbA (1.74 Å, PDB deposit code 2HHB; Fermi et al., 1984) using the program Insight II. Distances and angles were optimized by placing H 1.03 Å from the Tyr-O atom with ∠C−O−H = 109.5° and allowing the C-OH bond to swivel. [b] Tyr α24 has no hydrogen bonds in either the R- or T-states. [c] Calculated by placing an extra H 1.03 Å from the carboxylate O atom, oriented toward one of the Tyr O atom lone pairs (leading to alternative ∠ring-OH).

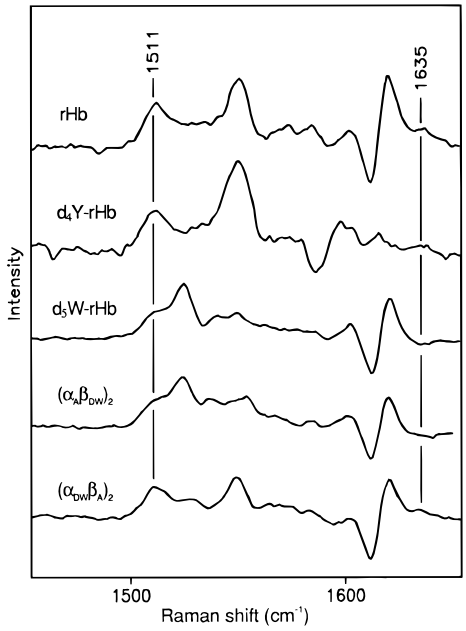

FIGURE 13: Expanded view of the difference spectra of rHb (natural abundance), rHb-Y-d_4, rHb-W-d_5, and the tryptophan isotope hybrids $(\alpha_A\beta_{DW})_2$ and $(\alpha_{DW}\beta_A)_2$, showing the 1511 cm^{-1} band unshifted upon Trp or Tyr labeling. Also shown is the weak W17 + W18 combination mode (1635 cm^{-1}), which was detected in all the difference spectra except for rHb-W-d_5 and the $(\alpha_A\beta_{DW})_2$ hybrid.

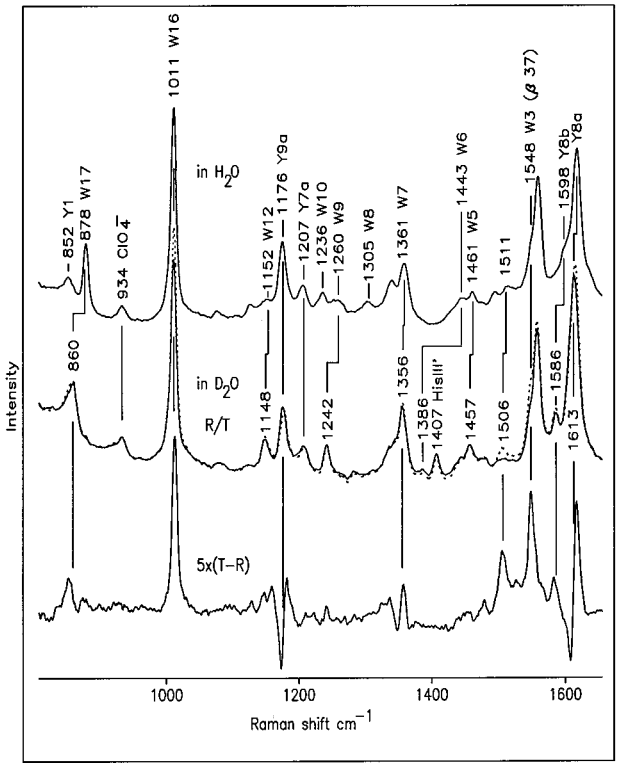

FIGURE 14: 229 nm excited UVRR spectra of HbA (T-state, dotted middle trace) and HbACO (R-state, solid middle trace) in D_2O (pD 7.4) and the T − R difference spectrum multiplied by a *y*-scale factor of 5 (bottom trace). Shown for comparison is the corresponding spectrum of HbACO (top trace) in H_2O (pH 7.4).

structurally homologous, and the Trp α14 T − R shifts of W17 and Wd5 are seen from the labeling experiments to be negligible.

Analysis of the crystallographic coordinates (Table 4) does suggest changes in the H-bond parameters for Trp α14 and β15. The Trp α14 H-bond appears to lengthen in the T-state, while the Trp β15 H-bond appears to shorten, although the R- and T-state distances are both quite long for Trp β15. However, the accuracy of these estimates, which require standard assumptions (Table 4) about the location of the (unobserved) H atoms, is suspect. We note that Trp β37 also appears to lengthen its H-bond in the T-state, a clearly unphysical result, since the H-bond acceptor is stronger in the T-state. We did not attempt energy minimization of the structures, which might have produced more reliable H-bond parameters.

The stronger Trp β37 H-bond can also account for the higher T-state intensities of the Trp bands since H-bond donation is known to shift the Trp excitation profile to the longer wavelengths, and therefore to increase the RR enhancement at 230 nm (Rodgers *et al.*, 1992). Consistent with this interpretation, the W3 T − R intensity difference is seen to be large for Trp β37 but small for both Trp α14 and Trp β15. For the remaining W*i* bands, the Trp β37 and β15 contributions are not resolved, but since the Trp α14 contributions are shown by the labeling results to be small in all cases, it is reasonable to infer that the Trp β15 contributions are also small and that the difference spectrum is dominated by Trp β37. This conclusion was also reached by Nagai *et al.* (1995) on the basis of T − R difference spectra for the Trp β37 mutant Hb Hirose.

We note that Nagai *et al.* (1995) proposed a different intensity mechanism, namely, a hypochromic ring-stacking interaction between Trp β37 and one of the nearby Tyr residues (Tyr β35, α42, and α140) in the R-state. Ring-stacking in nucleic acid helices is well-known to diminish RR intensity of purine and pyrimidine ring modes due to the absorption hypochromism induced by the stacking of the

bases (Grygon & Spiro, 1990; Fodor & Spiro, 1986), and similar interactions of aromatic rings are possible in proteins. However, analysis of the crystallographic coordinates of Hbs (Shaanan, 1983; Fermi *et al*., 1984) indicates that of the three nearby Tyr residues only Tyr α140 has its ring within 5 Å of the Trp β37 indole ring, and the dihedral angle between the two ring planes is not favorable for stacking (larger than ~70°) in either state. Consequently, the stacking mechanism is less likely than the H-bonding mechanism in accounting for the T-state intensification.

Switch. In the switch region of the subunit interface, an important H-bond is formed in the T-state between Tyr α42 and the side chain of Asp β99 (Perutz, 1990). Mutation of either residue [Yanase *et al*. (1994) and references therein] compromises the stability of the T-state, thereby raising the oxygen affinity and diminishing cooperativity in ligand binding. It has generally been assumed that the Tyr α42 OH group donates an H-bond to the ionized side chain of Asp β99. But a donor H-bond is inconsistent with the behavior of the Y8a and Y8b bands, which are expected to shift to lower frequencies upon H-bond donation from tyrosine (Hildebrandt *et al*., 1988). Instead Y8a and Y8b both shift to *higher* frequencies. It was therefore suggested (Rodgers *et al*., 1992) that Tyr α42 is an H-bond acceptor, instead of a donor, implying that the Asp β99 side chain is protonated, not ionized. The present results establish that the full 1.8 cm^{-1} upshift of Y8a occurs in the α-chains, presumably because of Tyr α42. This is evident from the spectra of the $(\alpha_A\beta_{DY})_2$ hybrid (Figure 11), in which the unlabeled Y8a is exclusively from the α-chains. In contrast, the $(\alpha_{DY}\beta_A)_2$ hybrid, in which only the β-chains are unlabeled, shows a Y8a intensity increase but *no* frequency shift in the T state. These results are consistent with recent site-mutant studies, in which no Y8a frequency shift was found in the T-state when Tyr α42 is replaced by His, leaving a His α42···Asp β99 H-bond (Nagai *et al*., 1996), or when Tyr α42 and Asp β99 are replaced by Asp and Asn respectively, leaving an Asp α42···Asn β99 H-bond (Huang *et al*., 1997). Thus, replacement of Tyr α42 eliminates the Y8a upshift observed in the T-state of Hb. It is clear that the Tyr α42 Y8a frequency is higher in the T- than in the R-state, whereas it would be lower if Tyr α42 were an H-bond donor.

We note that Cho *et al*. (1994) have argued for H-bond donation from Tyr α42 on the basis of their own UVRR data on fluoromet Hb, which showed that adding the T-state stabilizer inositol hexaphosphate produced (i) a slight red shift of the Y8a excitation profile and (ii) a downshift of a weak, broad band around 1260 cm^{-1}, which they assigned to Y7a′, a mode that is known (Takeuchi *et al*., 1989) to be sensitive to Tyr H-bond donation. However, Y7a′ is not enhanced with UV excitation between 217 and 250 nm (Ludwig & Asher, 1988; and see Figure 5), and the present labeling experiments clearly show the 1260 cm^{-1} band to be a Trp mode instead. Also, the red shift in the Y8a excitation profile cannot be due to Tyr α42, as the present results show that the Y8a intensity is unaltered in the α-chains; the T-state augmentation of intensity is due to the Tyr residues in the β-chains, and it is one or more of the β Tyr residues that give rise to the excitation profile red shift.

Thus, the RR evidence supports H-bond acceptance, not donation, by Tyr α42, implying that Asp β99 is protonated in the T state. Asp β99 protonation is also suggested by the Fourier transform infrared spectrum of Hb (Gregorious *et al*., 1995), which shows a 1697 cm^{-1} T − R difference band. This band is missing in the Dβ99N mutant Hb Kempsey and has been tentatively assigned to the C═O stretch of protonated Asp β99. However, the frequency is quite low for such a mode [possibly due to strong H-bonding (Gregoriou *et al*., 1995)], and the assignment awaits confirmation by isotope labeling.

The interpretation of the Tyr UVRR intensities is not straightforward. The β-chain residues collectively show enhanced Y8a intensity but diminished Y9a intensity in the T state, while the α-chain residues also show diminished Y9a intensity but unaltered Y8a intensity. Thus, these two Tyr modes response differently to the T-state environmental changes, implying different displacements of the Tyr excited states along the two normal coordinates. The three Tyr residues in each chain have different environmental changes (Table 5), making it impossible to attribute the net intensity differences to particular structural elements.

Histidine? Finally, we speculate on the origin of the 1511 cm^{-1} T-state marker band, which arises from neither Tyr nor Trp but possibly from His. This assignment is consistent with the direction of the T − R intensity change, since the candidate mode in aqueous histidine (~1500 cm^{-1}) intensifies upon imidazole protonation (Caswell & Spiro, 1986). Of the many His residues in Hb, several have higher pK_a values in the T-state than in the R-state (Ho & Russu, 1987). A prominent candidate is His β146, which has a substantial pK_a shift and contributes importantly to the alkaline Bohr effect, as revealed by chemical modification (Kilmartin & Wooton, 1970; Kilmartin *et al*., 1980) and mutation [for example, see Imai (1968) and Shih *et al*. (1993)] studies. Crystallographic studies also show that His β146 forms an intrasubunit salt bridge with Asp β94 in the T-state Hb (Fermi *et al*., 1984), and the bridge is broken in the R-state (Shaanan, 1983). Another possibility is that the signal arises from the proximal His residues (α87, β92) that ligate the heme Fe. The Fe−His(N_ϵ) bond is known to be strained in the T-state, especially in the α-chains, as evidenced by lowered frequencies of the Fe−His stretching vibration (Nagai & Kitagawa, 1980). In addition, the proximal His N_δH group is H-bonded to a backbone carbonyl (Bolton & Perutz, 1970; Ladner *et al*., 1977), and this H-bond may also be perturbed in the T-state. These T-state alterations of the imidazole bonding might shift the excitation profile to the red, producing the observed T-state Raman enhancement.

CONCLUSIONS

This study establishes the feasibility of chain-specific isotope labeling in Hb via expression of the gene in auxotrophic host strains of *E. coli* and reconstitution of functional tetramer from labeled and unlabeled chains. Tyrosine labeling has established that the strong T − R difference signal at *ca*. 1615 cm^{-1} is exclusively due to the Tyr Y8a mode with negligible contribution from the Trp (W1) or Phe (F8a) residues. Moreover, the Y8a upshift in the T-state is found to originate in the α subunits, supporting the previous inference that this shift is associated with the T-state H-bond involving the interfacial Tyr α42. These results are consistent with the interpretation that Tyr α42 accepts an H-bond from its partner Asp β99 in the T-state (Rodgers *et al*., 1992). Tryptophan labeling showed the Trp

α14 contribution to the T − R difference spectrum to be very small, indicating that the difference signals are dominated by Trp β37. This point was established definitely for the W3 band, whose position is shifted for Trp β37 relative to Trp β15. The observed downshift of W17 and upshift of Wd5 are consistent with a stronger Trp β37 H-bonding in the T-state than in the R-state, and the resulting excitation profile red shift accounts for the positive Trp intensity difference for all the Trp bands. Finally, the labeling results established that the important 1511 cm^{-1} difference band arises neither from Trp, as had previously been supposed (Rodgers *et al*, 1992), nor from Tyr, but possibly from a His residue.

ACKNOWLEDGMENT

We thank Professor Chien Ho for the generous gift of plasmid pHE2. We also thank Drs. Ishita Mukerji, George Heibel, William Simpson, Xiaojie Zhao, and Ragulan Ramanathan for helpful discussions. Drs. Mukerji and Heibel initiated the project, Dr. Simpson improved the performance of the Raman spectrometer, and Dr. Ramanathan obtained the mass spectra at the Washington University Mass Spectrometry Resource, NIH Research Resource (Grant P4 1RR0954). We also thank Beth Villafranca for creating Figure 1 and Professor Michael Hecht and Mr. Shoulian Dong for advice on protein expression.

REFERENCES

Antonini, E., & Brunori, M. (1971) in *Hemoglobin and Myoglobin and their Reactions with Ligands* (Neuberger, A., & Tatum, E. L., Eds.) pp 2−4, Elsevier, New York.
Austin, J., Jordan, T., & Spiro, T. G. (1993) in *Biomolecular Spectroscopy, Part A* (Clark, R. J. H., & Hester, R. E., Eds.) pp 55−125, John Wiley & Sons, New York.
Baldwin, J. (1980) *J. Mol. Biol. 130*, 103.
Baldwin, J., & Chothia, C. (1979) *J. Mol. Biol. 129*, 175.
Bollag, E. M., & Edelstein, S. J. (1991) in *Protein Methods*, pp 143−156, John Wiley & Sons, New York.
Bolton, W., & Perutz, M. F. (1970) *Nature (London) 228*, 551.
Cassoly, E., Gibson, Q. H. (1972) *J. Biol. Chem. 247*, 7332.
Caswell, D. S., & Spiro, T. S. (1986) *J. Am. Chem. Soc. 108*, 6470.
Cho, N., Song, S., & Asher, S. A. (1994) *Biochemistry 33*, 5932.
Copeland, R. A., & Spiro, T. G. (1985) *Biochemistry 24*, 4960.
Copeland, R. A., Dasgupta, S., & Spiro, T. G. (1985) *J. Am. Chem. Soc. 107*, 3370.
Fermi, G., Perutz, M. F., Shaanan, B., & Fourme, R. (1984) *J. Mol. Biol. 175*, 159.
Fodor, S. P. A., Copeland, R. A., Grygon, C. A., & Spiro, T. G. (1989) *J. Am. Chem. Soc. 111*, 5509.
Fodor, S. P., & Spiro, T. G. (1986) *J. Am. Chem. Soc. 108*, 3198.
Gregoriou, V. G., Jayaraman, V., Hu, X., & Spiro, T. G. (1995) *Biochemistry 34*, 6876.
Grygon, C. A., & Spiro, T. G. (1990) *Biopolymers 29*, 707.
Harada, I., Miura, T., & Takeuchi, H. (1986) *Spectrochim. Acta, Part A 42*, 307.
Harada, I., & Takeuchi, H. (1986) in *Advances in Infrared and Raman Spectroscopy* (Clark, R. J., & Hester, R. E., Eds.) Vol. 13, pp 113−173, John Wiley & Sons, New York.
Hildebrandt, P. G., Copeland, R. A., Spiro, T. G., Otlewski, J., Laskowski, M., & Prendergast, F. G. (1988) *Biochemistry 27*, 5426.
Hirsch, R. E., Lin, M. J., Vidugirus, G. V. A., Huang, S., Friedman, J. M., & Nagel, R. L. (1996) *J. Biol. Chem. 271*, 372.
Ho, C., & Russu, M. (1987) *Biochemistry 26*, 5426.
Hudson, B. S., & Mayne, L. C. (1987) in *Biological Applications of Raman Spectroscopy* (Spiro, T. G., Ed.) Vol. 3, pp 181−211, John Wiley & Sons, New York.
Huang, S., Peterson, E. S., Ho, C., & Friedman, J. M. (1997) *Biochemistry 36*, 6197.
Imai, K. (1968) *Arch. Biochem. Biophys. 127*, 543.
Ikeda-Saito, M., Inubushi, T., & Yonetani, T. (1981) *Methods Enzymol. 76*, 113.
Jayaraman, V., Rodgers, K. R., Mukerji, I., & Spiro, T. G. (1993) *Biochemistry 32*, 4547.
Jayaraman, V., Rodgers, K. R., Mukerji, I., & Spiro, T. G. (1995) *Science 269*, 1843.
Jayaraman, V., & Spiro, T. G. (1995) *Biochemistry 34*, 4511.
Jordan, T., & Spiro, T. G. (1995) *J. Raman Spectrosc. 26*, 867−876.
Jordan, T., Mukerji, I., Wang, Y., & Spiro, T. G. (1995) *J. Mol. Struct. 379*, 51.
Kilmartin, J. V., & Wootton, J. F. (1970) *Nature (London) 228*, 766.
Kilmartin, J. V., Fogg, J. H., & Perutz, M. F. (1980) *Biochemistry 19*, 3189.
Kitagawa, T. (1992) *Prog. Biophys. Mol. Biol. 58*, 1.
Ladner, R. C., Heidner, E. J., & Perutz, M. F. (1977) *J. Mol. Biol. 114*, 385.
Laskowski, R. A., MacArthur, M. W., Moss, D. S., & Thornton, J. M. (1993) *J. Appl. Crystallogr. 26*, 283.
LeMaster, D. M., & Richards, F. M. (1985) *Biochemistry 24*, 7263.
LeMaster, D. M., & Richards, F. M. (1988) *Biochemistry 27*, 142.
Liu, G.-y., Grygon, C. A., & Spiro, T. G. (1989) *Biochemistry 28*, 5046.
Looker, D., Mathews, A. J., Neway, J. O., & Stetler, G. L. (1994) *Methods Enzymol. 231*, 364.
Ludwig, M., & Asher, S. A. (1988) *J. Am. Chem. Soc. 110*, 1005.
Maruyama, T., & Takeuchi, H. (1995) *J. Raman Spectrosc. 26*, 319.
Miura, T., Takeuchi, H., & Harada, I. (1988) *Biochemistry 27*, 88.
Miura, T., Takeuchi, H., & Harada, I. (1989) *J. Raman Spectrosc. 20*, 667.
Mukerji, I., & Spiro, T. G. (1995) *Biochemistry, 33*, 13132.
Nagai, M., Imai, K., Kaminaka, S., Mizutani, Y., & Kitagawa, T. (1996) *J. Mol. Struct. 379*, 65.
Nagai, M., Kaminaka, S., Ohba, Y., Nagai, Y., Mizutani, Y., & Kitagawa, T. (1995) *J. Biol. Chem. 270*, 1636.
Nagai, K., & Kitagawa, T. (1980). *Proc. Natl. Acad. Sci. U.S.A. 77*, 2033.
Perutz, M. F. (1990) *Annu. Rev. Physiol. 52*, 1−25.
Rava, R. P., & Spiro, T. G. (1985) *J. Phys. Chem. 89*, 1856.
Rodgers, K. R., Su, C., Subramaniam, S., & Spiro, T. G. (1992) *J. Am. Chem. Soc. 114*, 3697.
Rodgers, K. R., & Spiro, T. G. (1994) *Science 265*, 1697.
Salama, S., & Spiro, T. G. (1978) *J. Am. Chem. Soc. 100*, 1105.
Shaanan, B. (1983) *J. Mol. Biol. 171*, 31.
Shen, T.-J., Ho, N. T., Simplaneaun, V., Zou, M., Green, B. N., Tam, M. F., & Ho, C. (1993) *Proc. Natl. Acad. Sci. U.S.A. 90*, 8108.
Shil, D. T.-b., Luisi, B. F., Miyazaki, G., Perutz, M. F., & Nagai, K. (1993) *J. Mol. Biol. 230*, 1291.
Song, S., Asher, S. A., Krimm, S., & Shaw, K. D. (1991) *J. Am. Chem. Soc. 113*, 1155.
Su, C., Park, Y. D., Liu, G. Y., & Spiro, T. G. (1987) *J. Am. Chem. Soc. 111*, 3457.
Takeuchi, H., & Harada, I. (1986) *Spectrochim. Acta 42A*, 1069.
Takeuchi, H., & Harada, I. (1990) *J. Raman Spectrosc. 21*, 509.
Takeuchi, H., Watanabe, N., & Harada, I. (1988) *Spectrochim. Acta. 44A*, 749.
Takeuchi, H., Watanabe, N., Satoh, U., & Harada, I. (1989) *J. Raman Spectrosc. 20*, 565.
Yanase, H., Cahill, S., Martin de Llano, J. J., Manning, L. R., Schneider, K., Chait, B. T., Vandegriff, K. D., Winslow, R. M., & Manning, J. M. (1994) *Protein Sci. 3*, 1213.

BI971136L